# $CS_2$ Fixation by Carbonic Anhydrase Model Systems—A New Substrate in the Catalytic Cycle

**Sebastian Sinnecker,[†] Michael Bräuer,[‡] Wolfram Koch,*[,§] and Ernst Anders*[,‡]**

Institut für Organische Chemie der Technischen Universität Berlin, Strasse des 17. Juni 135, D-10623 Berlin, Germany, and Institut für Organische Chemie und Makromolekulare Chemie der Friedrich-Schiller-Universität Jena, Humboldtstrasse 10, D-07743 Jena, Germany, and Gesellschaft Deutscher Chemiker, Varrentrappstrasse 40-42, D-60486 Frankfurt am Main, Germany

*Received October 17, 2000*

The conversion of $CS_2$ with common carbonic anhydrase model systems has been studied using Hartree−Fock and density-functional theory methods employing the 6-311+G* basis set. The calculated geometries and energetical parameters for $[L_3ZnOH]^+/CS_2$ model systems (L = $NH_3$, imidazole) are compared with those obtained previously for the $CO_2$ hydration. While the same reaction mechanism applies for both heterocumulenes, the hypothetical conversion of $CS_2$ to give $[L_3ZnSC(O)SH]^+$ is characterized by a higher barrier and is much more exothermic than the corresponding $CO_2$ reaction cascade. Due to the increased number of heteroatoms, additional intermediates and product structures (compared with those involved in the $CO_2$ conversion) must be taken into account and have been analyzed in detail. The smaller electrophilicity of $CS_2$ is the reason for the higher activation energies, while the significantly increased exothermicity is due to the strong zinc(II)/sulfur interaction. The reversibility and therefore the existence of a catalytic cycle which could allow comparable $CS_2$ transformations must be questioned. Nevertheless, an interesting field of stoichiometric zinc-mediated $CS_2$ transformations is conceivable.

## 1. Introduction

The importance of zinc in biochemistry has been illuminated in detail by various authors. Besides the function of zinc in carbonic anhydrase, alcoholic dehydrogenases, and carboxypeptidase, this metal is also of importance in the photochemistry of vision.[1−10]

The enzyme carbonic anhydrase (CA) has been isolated by Meldrum and Roughton,[11] and the structures of the human isoenzymes have been elucidated by various X-ray studies.[12−15] Such detailed high-resolution investigations are often a convenient starting point for theoretical studies.

The enzyme catalyzes the hydration of carbon dioxide with tremendous turn over numbers between $10^3$ and $10^6$ $s^{-1}$.[16−18] By the time the structure of the active site had been obtained, mechanisms had been proposed for the catalytic cycle and verified using experiments[19−24] as well as theoretical methods,[25−29] quoting only some leading references. There is no doubt that the first step is the deprotonation of zinc-bound water (Scheme 1). The metal reduces the p$K_a$ value of water drastically and hence permits this step under physiological pH conditions. The nucleophilic zinc-bound hydroxide attacks the carbon dioxide, which is strongly polarized by the metal and the surrounding medium. However, in computational investigations where the protein environment is neglected, the appropriate product of this step differs from the suggestion accepted over the past years.[30−32]

* Authors for correspondence.
[†] Technischen Universität Berlin.
[‡] Friedrich-Schiller-Universität Jena.
[§] Gesellschaft Deutscher Chemiker.

(1) Prince, R. H. *Adv. Inorg. Chem. Radiochem.* **1979**, *22*, 349.
(2) Vahrenkamp, H. *Bioinorganic Chemistry*; *Coordination Chemistry of Zinc Related to an Understanding of its Biological Functions*; Wiley-VCH: 1997; p 540.
(3) Vallee, B. L.; Auld, D. S. *Acc. Chem. Res.* **1993**, *26*, 543.
(4) Lipscomb, W. N.; Sträter, N. *Chem. Rev.* **1996**, *Vol. 96*, *7*, 2376.
(5) Vanhommerig, S. A. M.; Meier, R. J.; Sluyterman, A. Æ.; Meijer, E. M. *J. Mol. Struct. (THEOCHEM)* **1996**, *33*, 364.
(6) Lesburg, C. A.; Christianson, D. W. *J. Am. Chem. Soc.* **1995**, *117*, 6838.
(7) Ritter, A. v. O.; Clark, T. *J. Comput. Chem.* **1993**, *14*, *4*, 392.
(8) Alex, A.; Clark, T. *J. Comput. Chem.* **1992**, *13*, *6*, 704.
(9) Valle, B. L.; Auld, D. S. *Biochemistry* **1990**, *29*, 5647.
(10) Lipscomb, W. N. *Annu. Rev. Biochem.* **1983**, *52*, 17.
(11) Meldrum, N. U.; Roughton, F. J. W. *J. Physiol. (London)* **1932**, *75*, 15.
(12) Kannan, K. K.; Liljas, A.; Vaara, I.; Bergsten, P.-C.; Lövgren, S.; Strandberg, B.; Bengston, U.; Carlboom, U.; Fridborg, K.; Järup, L.; Petef, M. *Cold Spring Harbor Symp. Quantum Biol.* **1971**, *36*, 221.
(13) Kannan, K. K.; Nostrand: B.; Fridborg, K.; Lövgren, S.; Ohlsson, A.; Petef, M. *Proc. Natl. Acad. Sci. U.S.A.* **1975**, 72, 51.
(14) Vaara, I.; Lövgren, S.; Liljas, A.; Kannan, K. K.; Bergsten, P.-C. *Adv. Exp. Med. Biol.* **1972**, *28*, 169.
(15) Liljas, A.; Kannan, K. K.; Bergsten, P.-C.; Vaara, I.; Fridborg, K.; Strandberg, B.; Carlbom, U.; Järup, L.; Lövgren, S.; Petef, M. *Nature (London), New Biol.* **1972**, *235*, 131.
(16) Khalifah, R. G. *J. Biol. Chem.* **1971**, *246*, 2561.
(17) Steiner, H.; Jönsson, B.-H.; Lindskog, S. *Eur. J. Biochem.* **1975**, *59*, 253.
(18) Sanyal, G.; Swenson, E. R.; Pessah, N. I.; Maren, T. H. *Mol. Pharmacol.* **1982**, *22*, 211.
(19) Zhang, X.; Hubbard, C. D.; van Eldik, R. *J. Phys. Chem.* **1996**, *100*, 9161.
(20) Silverman, D. N.; Lindskog, S. *Acc. Chem. Res.* **1988**, *21*, 30.
(21) Liang, J.-Y.; Lipscomb, W. N.; *J. Am. Chem. Soc.* **1986**, *108*, 5051.
(22) Simonson, I.; Jonsson, B.-H.; Lindskog, S. *Eur. J. Biochem.* **1979**, *93*, 409.
(23) Demoulin, D.; Pullman, A. *Theor. Chim. Acta* **1978**, *49*, 161.
(24) Pocker, Y.; Deits, T. L.; *J. Am. Chem. Soc.* **1983**, *105*, 980.
(25) Solà, M.; Lledós, A.; Duran, J.; Bertrán, J. *J. Am. Chem. Soc.* **1992**, *114*, 869.
(26) Merz, Jr., K. M.; Hoffmann, R.; Dewar, M. J. S. *J. Am. Chem. Soc.* **1989**, *111*, 5636.
(27) Lu, D.; Voth, G. A. *J. Am. Chem. Soc.* **1998**, *120*, 4006.
(28) Krauss, M.; Garmer, D. R.; *J. Am. Chem. Soc.* **1991**, *113*, 6426.
(29) Hartmann, M.; Clark, T.; van Eldik, R. *J. Mol. Model.* **1996**, *2*, 1.
(30) Zheng, Y.-J.; Kenneth, M.; Merz, Jr. *J. Am. Chem. Soc.* **1992**, *114*, 10498.

10.1021/ic001149e CCC: $20.00 
Published on Web 02/02/2001

**Scheme 1.** The Proposed Catalytic Cycle of the Carbonic Anhydrase (L = Histidine), Considering the Results of Recent Quantum Chemical Calculations with Model Systems (L = $NH_3$, Imidazole)

1. Deprotonation of zinc bound water

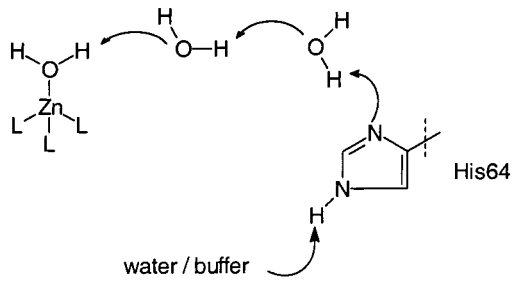


2. Nucleophilic attack

3. Isomerization

a) Lipscomb pathway (proton transfer):

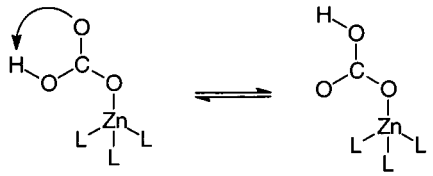

b) Lindskog like pathway (bond rotation):

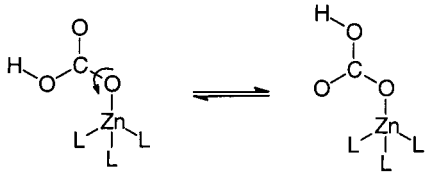

4. Displacement of hydrogencarbonate with water

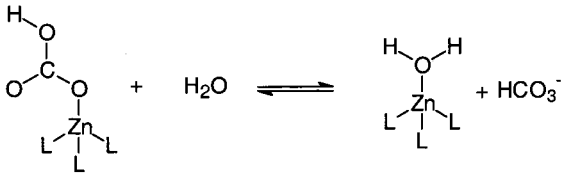


This leads to slightly different isomerization reactions, also displayed in Scheme 1. Whereas there is still a proton-transfer conceivable as suggested by Lipscomb et al.,[33] the proposed pathway of Lindskog and co-workers[34] might be described by rotation along the bond between the carbon and the zinc-bound oxygen. The last step is the replacement of the metal-coordinated hydrogen carbonate by a water molecule to prepare the system for a further catalytic cycle.

Regarding a quantum chemical description of this reaction, many studies have been performed.[25−32] However, due to limited computing resources, these were often restricted to smaller model systems, semiempirical methods, or ab initio approaches using only limited basis sets. Among the more recent investigations we note the contribution by Garmer,[35] who modeled the enzymatic step, including the environment through an effective interaction model. In the present study our main focus is, however, not the real enzyme, rather we concentrate on related, but artificial, systems.

The substitution of oxygen in $CO_2$ by sulfur leads to $CS_2$. Since both elements are in the same group of the periodic table, similar reactions are to be expected. And indeed, while for example the reaction of $CO_2$ with Grignard reagents leads to esters, $CS_2$ is transformed into thioesters. Likewise it is possible to transform amines in the presence of a base into thiocarbamates with $CS_2$, akin to the corresponding transformation of amines into carbamates through $CO_2$. Apart from these similarities some properties of sulfur let us expect also deviations from the CA-type reaction. Especially the lower electrophilicity and the higher polarizability of sulfur should lead to a different coordination behavior of $CS_2$ as compared to $CO_2$.

The present study computationally examines the hydration of $CS_2$ by the common $[(NH_3)_3ZnOH]^+$ and $[(Imi)_3ZnOH]^+$ model systems (Imi = imidazole) in comparison to the corresponding conversion of $CO_2$ (nucleophilic attack and the isomerization step). To this end we employ Hartree−Fock (HF) and density functional theory based approaches (DFT) combined with basis sets of adequate quality. To the best of our knowledge, the hydration of $CS_2$ by carbonic anhydrase model systems has not yet been investigated by quantum chemical methods, while experimental investigations using pyrazolylborate−zinc model complexes were carried out by Vahrenkamp et al. A combined experimental/theoretical investigation regarding the applicability has been presented recently.[36]

We will present the mechanisms for the conversion of $CS_2$ using the same model systems and level of theory as employed recently by Anders and co-workers for the $CO_2$ hydration.[32] This strategy permits detailed comparisons for the two substrates.

## 2. Computational Methods

The standard triple-$\zeta$ 6-311+G* basis set,[37] which includes polarization and diffuse functions on all non-hydrogen atoms, was employed throughout. For Zn this translates into a McLean/Chandler basis set.[38] Due to the closed-shell character of the complexes and the $d^{10}$ configuration of the metal, even the uncorrelated HF approach is expected to give reasonable results. To obtain more accurate data, electron correlation effects have been included through approximate density functional theory.[39−42]

(31) Muguruma, C. *J. Mol. Struct. (THEOCHEM)* **1999**, *461−462*, 439.
(32) Bräuer, M.; Perez-Lustres, J. L.; Anders, E. Manuscript in preparation.
(33) Liang, J.-Y.; Lipscomb, W. N. *Int. J. Quantum Chem.* **1989**, *36*, 299.
(34) Lindskog, S.; Engberg, P.; Forsman, C.; Ibrahim, S. A.; Jönsson, B.-H.; Simonsson, I.; Tibell, L. *Annals New York Academy of Science*; Tashian, R. E., Hewett-Emmett, D., Eds.; The New York Academy of Science: New York, 1984; Vol. 429, p 61.
(35) Garmer, D. R. *J. Phys. Chem. B* **1997**, *101*, 2945.
(36) Bräuer, M.; Anders, E.; Sinnecker S.; Koch, W.; Rombach, M.; Vahrenkamp, H. *Chem. Commun.* **2000**, 637.
(37) Krishnan, R.; Binkley, J. S.; Seeger, R.; Pople, J. A. *J. Chem. Phys.* **1980**, *72*, 650.
(38) McLean, A. D.; Chandler, G. S. *J. Chem. Phys.* **1980**, *72*, 5639.
(39) Koch, W.; Holthausen, M. C. *A Chemist's Guide to Density Functional Theory*; Wiley-VCH: Weinheim, 2000.
(40) Hohenberg, P.; Kohn, W. *Phys. Rev. B* **1964**, *136*, 864.
(41) Kohn, W.; Sham, L. *Phys. Rev. A* **1965**, *140*, 1133.
(42) Parr, R. G.; Yang, W. *Density-Functional Theory of Atoms and Molecules*; Oxford University Press: Oxford, 1989.

We used the popular B3LYP hybrid approach,[43−46] which proved to yield reliable results in numerous fields, including transition metal applications.[39,47]

Frequency calculations for all stationary points verified their character as minima or saddle points and enabled the estimation of zero point energy (ZPE) corrections, which are included without scaling in all relative energies. Atomic net charges used in the discussion are natural charges obtained from natural bond order (NBO) calculations.[48] For the small systems relevant in the uncatalyzed reaction, coupled cluster calculations at the CCSD(T)/6-311+G*//B3LYP/6-311+G* level of theory[49,50] were employed as a reference.

All calculations have been performed by employing the Gaussian 94[51] and 98[52] program packages.

## 3. Results and Discussion

**3.1. Uncatalyzed Hydration of $CS_2$ and Sulfur−Zinc Interaction.** In contrast to $CO_2$, the negative net charge in $CS_2$ is located on the carbon atom. A CCSD(T)/6-311+G*//B3LYP/6-311+G* calculation determined a carbon partial charge of −0.28. This fact is only at first glimpse surprising. Considering the formal sp-hybridization of carbon in heterocumulenes, a Mulliken electronegativity[53,54] of 3.29 must be assigned to this atom in its bound state. This value is larger than for sulfur, which causes the shift of the electron density toward the center of the molecule. However, the small differences in electronegativity between oxygen and sulfur make a nucleophilic attack still conceivable.

As depicted in Scheme 2, the nucleophilic attack of $OH^-$ at $CS_2$ proceeds without activation energy and results in a product, stabilized by −57.4 kcal/mol, which is 12.4 kcal/mol more stable than the corresponding product from the reaction with carbon dioxide (−45.0 kcal/mol).[32] The greater polarizability of sulfur allows for a better distribution of the negative charge over the whole molecule. This reduces the electrostatic repulsion, especially between the central carbon atom and the oxygen bound hydrogen atom. The system is further stabilized by 6.5 kcal/mol through migration of a hydrogen from oxygen to sulfur. The exothermic character of this last step can be explained by negative hyperconjugation due to overlap of a heteroatom lone pair with a vicinal $\sigma^*$ orbital between a carbon and a further heteroatom.[55−58] This interaction is stronger in the case of oxygen than for sulfur. It is further strengthened for atoms not being protonated.

The reactions of both $CO_2$ and $CS_2$ with water are characterized by high barriers in the gas phase (Scheme 3). For $CS_2$ a barrier of 52.3 kcal/mol results at CCSD(T)/6-311+G*//B3LYP/6-311+G*, whereas a somewhat higher value of 62.1 kcal/mol is determined for $CO_2$. The reduced electropositive character of the carbon in $CS_2$ with respect to $CO_2$ should increase the barrier on one hand. On the other hand, the repulsive interactions in the transition structures are lowered in the case of $CS_2$, which decreases the barrier. The second assumption is supported by the geometries of the transition structures (Figure 1), which show a much closer contact between the hydrogen and the central carbon in the case of $CO_2$. Since the two effects act in opposite directions, they partially cancel each other and only small differences in the activation energies for the reactions of both substrates with water result.

**Scheme 2.** The Reaction of the Negatively Charged System $OH^- + CS_2$, Relative Energies (kcal/mol), and NBO Net Charges at the CCSD(T)/6-311+G*//B3LYP/6-311+G* Level of Theory

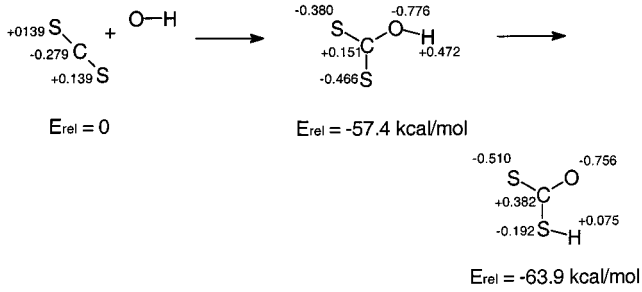


**Scheme 3.** Relative Energies for the Reaction of $CS_2$ and $CO_2$ (X = S or O) with Water at the CCSD(T)/6-311+G*//B3LYP/6-311+G* Level of Theory[a]

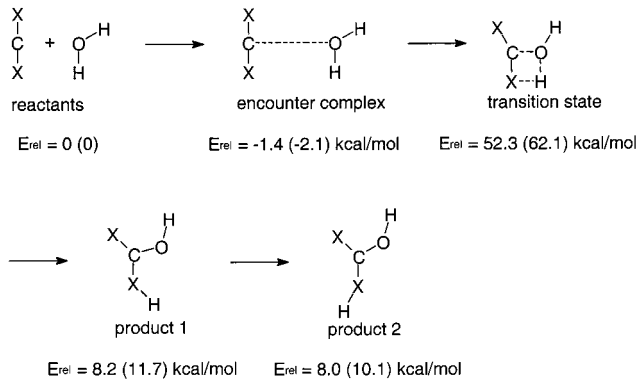


[a] The values for $CO_2$ are given in parenthesis

(43) Devlin, P. J.; Chabalowski, F. J.; Frisch, M. J. *J. Phys. Chem*. **1994**, *98*, 11623.
(44) Lee, C.; Yang, W.; Parr, R. G. *Phys. Rev. B* **1988**, *37*, 785.
(45) Becke, A. D. *J. Chem. Phys*. **1993**, *98*, 1372.
(46) Becke, A. D. *Phys. Rev. B* **1988**, *38*, 3098.
(47) Koch, W.; Hertwig, R. H. Density Functional Theory Applications to Transition Metal Problems. In *The Encyclopedia of Computational Chemistry*; Schleyer, P. v. R., Ed.-in-chief; Wiley: New York, 1998.
(48) Glendening, E. D.; Reed, A. E.; Carpenter, J. E.; Weinhold, F. NBO Version 3.1, as implemented in Gaussian 94 and 98.
(49) Scuseria, G. E.; Lee, T. J. *J. Chem. Phys*. **1990**, *93*, 5851.
(50) Watts, J. D.; Gauss, J.; Bartlett, R. J. *J. Chem. Phys*. **1993**, *98*, 8718.
(51) Frisch, M. J.; Trucks, G. W.; Schlegel, H. B.; Gill, P. M. W.; Johnson, B. G.; Robb, M. A.; Cheeseman, J. R.; Keith, T. A.; Petersson, G. A.; Montgomery, J. A.; Raghavachari, K.; Al-Laham, M. A.; Zakrzewski, V. G.; Ortiz, J. V.; Foresman, J. B.; Cioslowski, J.; Stefanov, B., B.; Nanayakkara, A.; Challacombe, M.; Peng, C. Y.; Ayala, P. Y.; Chen, W.; Wong, M. W.; Andres, J. L.; Replogle, E. S.; Gomperts, R.; Martin, R. L.; Fox, D. J.; Binkley, J. S.; DeFrees, D. J.; Baker, J.; Stewart, J. P.; Head-Gordon, M.; Gonzales, C.; Pople, J. A. *Gaussian 94*; Gaussian, Inc.: Pittsburgh, PA, 1995.
(52) Frisch, M. J.; Trucks, G. W.; Schlegel, H. B.; Scuseria, G. E.; Robb, M. A.; Cheeseman, J. R.; Zakrzewski, V. G.; Montgomery, J. A.; Stratmann, R. E.; Burant, J. C.; Dapprich, S.; Millam, J. M.; Daniels, A. D.; Kudin, K. N.; Strain, M. C.; Farkas, O.; Tomasi, J.; Barone, V.; Cossi, M.; Cammi, R.; Mennucci, B.; Pomelli, C.; Adamo, C.; Clifford, S.; Ochterski, J.; Petersson, G. A.; Ayala, P. Y.; Cui, Q.; Morokuma, K.; Malick, D. K.; Rabuck, A. D.; Raghavachari, K.; Foresman, J. B.; Cioslowski, J.; Ortiz, J. V.; Stefanov, B. B.; Liu, G.; Liashenko, A.; Piskorz, P.; Komaromi, I.; Gomperts R.; Martin, R. L.; Fox, D. J.; Keith, T.; Al-Laham, M. A.; Peng, C. Y.; Nanayakkara, A.; Gonzales, C.; Challacombe, M.; Gill, P. M. W.; Johnson, B. G.; Chen, W.; Wong, M. W.; Andres, J. L.; Head-Gordon, M.; Replogle, E. S.; Pople, J. A. *Gaussian 98*; Gaussian, Inc.: Pittsburgh, PA, 1998.
(53) Hinze, J.; Jaffè, H. H. *J. Am. Chem. Soc*. **1962**, *84*, 540.
(54) Hinze, J.; Jaffè, H. H. *J. Phys. Chem.* **1963**, *67*, 1501.
(55) Nordhoff, K.; Anders, E. *J. Org. Chem.* **1999**, *64*, 7485−7491.
(56) Juaristi, E. *Conformational Behavior of Six-Membered Rings: Analysis, Dynamics, and Stereoelectronic Effects*; VCH Publishers: New York, 1995.
(57) Juaristi, E. *Introduction to Stereochemistry and Conformational Analysis*; John Wiley & Sons: New York, 1991.
(58) Deslongchamps, P. *Stereoelectronic Effects in Organic Chemistry*; Pergamon Press: Oxford, 1984.

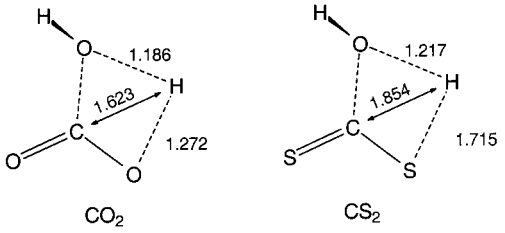


**Figure 1.** The transition structures of the nucleophilic attack for the uncatalyzed reaction of water with $CO_2$ and $CS_2$ at the B3LYP/6-311+G* level of theory; bond distances in Å.

**Scheme 4.** The Hydration of $CS_2$ by the $ZnOH^+$ Model System[a]

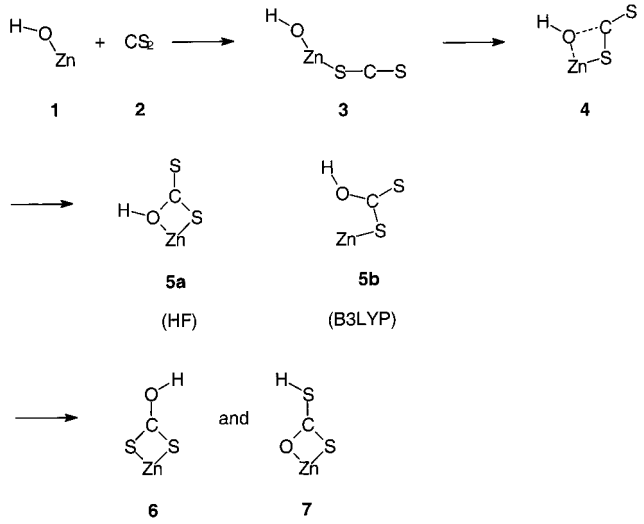


[a] The B3LYP and HF optimizations yielded very similar structures. However, strong distinctions could be determined for the product of the nucleophilic attack **5**: while the HF calculation yielded the ring structure **5a**, the oxygen−zinc bond is broken in the B3LYP-optimized structure **5b**.

To get an idea about the order of magnitude of heterocumulene−zinc interaction energies, the simplest model, i.e., $[Zn{-}X{=}C{=}X]^{2+}$ complexes with X = O or S, were employed to calculate the corresponding dissociation energies. The results obtained at the CCSD(T)/6-311+G*//B3LYP/6-311+G* level of theory predict an interaction energy of 126.5 kcal/mol for $CS_2$, while a much smaller value of 69.3 kcal/mol was obtained for $CO_2$.[32] This strong interaction of the sulfur-containing cumulene questions the applicability of the mechanism of the CA-reaction for this substrate, because a precoordination between zinc and sulfur is more likely than a zinc−oxygen interaction as established for the hydration of carbon dioxide. Provided that the ligand sphere of the metal does not prevent a coordination between zinc and sulfur, the nucleophilic attack of zinc-bound hydroxide to $CS_2$ would not be the first reaction step, but rather the formation of a zinc−sulfur bond.

**3.2. Hydration of $CS_2$ by the $Zn{-}OH^+$ Complex.** Although this complex is not of practical relevance, it permits the comparison of the energies determined at the B3LYP/6-311+G* level of theory with the corresponding CCSD(T)/6-311+G* energies based on B3LYP/6-311+G* and HF/6-311+G* optimized geometries, respectively. The structures investigated are displayed in Scheme 4. Since qualitatively the same species appear along the reaction path of the conversion of $CS_2$ with the tetrahedral coordinated metal (Scheme 5), the same numbering has been chosen in order to simplify the comparison. For example, **1** always represents the hydroxylated Zn system, **3** the encounter complex between **1** and the substrate, etc. From

**Scheme 5.** The Proposed Hydration of $CS_2$, Based on a Schematic Replacement of $CO_2$ with $CS_2$[a]

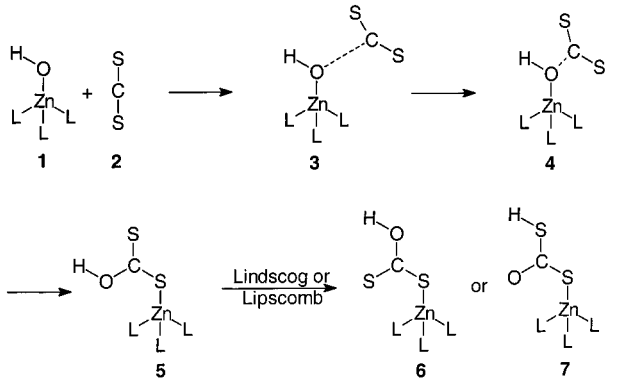


[a] The reactants **1** and **2** form an encounter complex **3**, the transition structure of the nucleophilic attack **4**, and the corresponding product **5**. A further isomerization leads to the structures **6** (Lindskog-like pathway) and **7** (Lipscomb mechanism)

**Table 1.** Relative Energies for the Stationary Points of the Reaction of $Zn{-}OH^+$ with $CS_2$ as Depicted in Scheme 4[a]

| | 1 + 2 | 3 | 4 | 5 | 6 | 7 |
|---|---|---|---|---|---|---|
| B3LYP | 0 | −50.0 | −20.2 | −28.4 | −46.8 | −42.4 |
| HF | 0 | −44.4 | −13.1 | −26.3 | −52.1 | −47.7 |
| CCSD(T)//B3LYP | 0 | −54.6 | −24.5 | −24.6 | −50.2 | −44.9 |
| CCSD(T)//HF | 0 | −54.4 | −25.1 | −29.0 | −49.9 | −44.8 |

[a] All calculations employ the 6-311+G* basis set. Energies in kcal/mol, including ZPEs.

the context it will be clear to which actual system the number refers to. The hydration of $CS_2$ commences with the exothermic coordination of sulfur to zinc (see Table 1: −50.0 and −54.6 kcal/mol at B3LYP and CCSD(T)//B3LYP levels of theory, respectively, with respect to the separated reactants). The following nucleophilic attack is characterized by a barrier of 29.9 (30.1) kcal/mol (transition structure **4** in Scheme 4). However, for the relative energy of the corresponding product, the two methods are in only disappointing agreement with each other. At B3LYP the formation of **5b** is characterized by an energy gain of −8.2 kcal/mol with respect to transition structure **4**, while the corresponding CCSD(T) value is effectively zero, namely −0.1 kcal/mol. However, it must be pointed out that the optimizations at B3LYP and HF yield different products for this step. While at HF a four-membered ring structure (**5a**) is predicted, this minimum does not exist at the B3LYP level of theory. Rather, the DFT calculations detected only a minimum where the oxygen−zinc bond is broken, i.e., **5b**. The CCSD(T) single-point energies indicate that the coupled cluster approach favors the HF-optimized reaction product **5a**. Actually this structure is the only case where the CCSD(T)//HF total energy is lower than the CCSD(T)/B3LYP result. At first glance this discrepancy might appear to be problematic, but as we will discuss further below, the HF and B3LYP optimizations yield very similar geometries for the $[(NH_3)_3ZnOH]^+$ complex. Hence, the different structures of **5a** and **5b** seem to be a unique problem of this particular species. Proceeding further along the $CS_2 + ZnOH^+$ reaction coordinate two additional products, **6** and **7** (Scheme 4), have been identified. In both cases the B3LYP and CCSD(T)//B3YLP results where again in good agreement with each other, both with respect to the computed geometries and the relative energies with differences of 3.4 and 2.5 kcal/mol, respectively (Table 1). From this comparison we can conclude that the more accurate CCSD(T) relative energies do not differ significantly from their B3LYP counterparts. Our

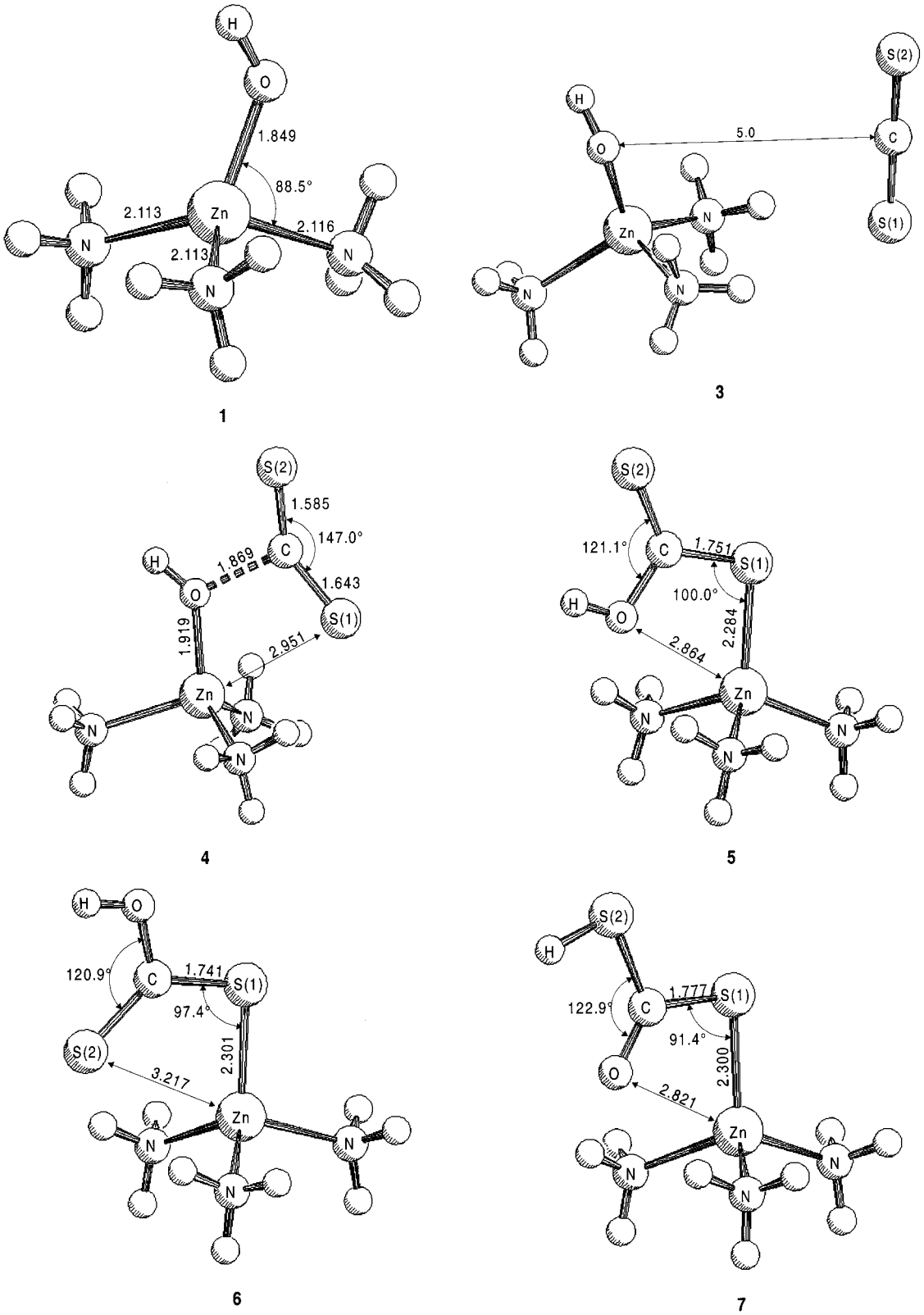


**Figure 2.** $CS_2$ conversion through the $[(NH_3)_3ZnOH]^+$ model, displaying the optimized structures at the B3LYP/6-311+G* level of theory: Reactant complex **2a**, encounter complex **2b**, transition structure of the nucleophilic attack **2c**, the corresponding product **2d,** as well as the Lindskog and Lipscomb isomers **2e** and **2f**.

strategy of using B3LYP energies rather than the very expensive CCSD(T) ones will hence introduce only small errors on the order of some 5 kcal/mol, which will not change the qualitative conclusions of our study.

**3.3. $CS_2$ Conversion through the $[(NH_3)_3ZnOH]^+$ Model.** A formal replacement of $CO_2$ with $CS_2$ in the CA-catalytic cycle leads to the structures displayed in Scheme 5. The presence of the heteroatoms in the substrate causes the Lindskog and Lipscomb pathways now to yield different isomers. As already outlined above, the same numbering from **1** to **7** as introduced in the preceding paragraph will be used to name the various intermediates and saddle points along the reaction coordinate.

As indicated by a comparison between Schemes 4 and 5, the structures in this and the following paragraphs are always characterized by a Zn center carrying three ligands L (with L = $NH_3$, imidazole), while before no such ligands were present. The optimized geometries of all relevant species have been collected in Figure 2.

The structure of the free catalyst **1** is characterized at the B3LYP/6-311+G* level of theory by metal−nitrogen bond distances between 2.11 and 2.12 Å. Comparing the HF- and B3LYP-optimized structures reveals that the density functional calculations result in slightly shorter N−Zn bonds, a longer oxygen−metal bond, and a more distorted tetrahedral coordination of the zinc cation.

The encounter complex **3** is stabilized with respect to the reactants by 2.1 (HF) and 2.5 (B3LYP) kcal/mol, respectively. The large separation of the reactants in comparison to the encounter complexes found for $CO_2$ in the work of Bräuer et al.[32] might be explained by a less electrophilic substrate due to the pronounced polarizability of sulfur.

The transition structure **4** for the nucleophilic attack leads to barriers of 18.2 kcal/mol at the HF/6-311+G* level of theory and 14.3 kcal/mol for the B3LYP/6-311+G* optimization. The distances between oxygen and the carbon atoms amount to 1.908 Å in the HF calculation and to 1.869 Å in the B3LYP calculation. In both cases, the $CS_2$ moiety is bent with unequal sulfur−carbon bond lengths. The larger value was found for the C−S(1) bond pointing to the metal and the ammonia ligands. The increased negative net charge of S(1) (−0.14 instead of +0.18 for S(2) at the B3LYP level) amplifies the attractive Coulomb interaction between zinc and S(1). The substrate is polarized, a well-known effect of the $CO_2$ hydration. Here, as well as for the next structures, the HF and B3LYP geometries using the 6-311+G* basis set are very similar. The short distance between zinc and sulfur S(1) during the nucleophilic attack indicates the displacement of the protonated oxygen by sulfur. This straightforwardly results in structure **5** with sulfur S(1) coordinated to the metal. The imaginary modes of the HF as well as the B3LYP transitions structures show no components between zinc and sulfur S(1). An intrinsic reaction coordinate (IRC) calculation[59−61] at the HF/6-311+G* level of theory provides the following picture: in the first step the carbon oxygen bond is completely formed, subsequently followed by an activationless displacement of the metal coordinated oxygen with sulfur S(1). The reaction is exothermic by 11.0 (HF) and 5.4 (B3LYP) kcal/mol, respectively.

Considering the principles of the Lindskog and Lipscomb mechanisms, the reaction can proceed further to give two different structures, **6** and **7** (Scheme 5). In the case of $CO_2$, these product structures are identical. The introduction of heteroatoms leads to structure **6**, with two sulfur atoms interacting with zinc (HF, −19.4 kcal/mol; B3LYP, −10.9 kcal/mol, with respect to the separated reactants), which is brought about by an internal rotation around the C−S(1) bond. This structural motif can be considered as the insertion product of $CS_2$ into a Zn−O bond and was for example found in Cd−phenoxide complexes.[62] An internal proton transfer between the oxygen and the sulfur in structure **5** leads to the product **7** (HF, −28.7 kcal/mol; B3LYP, −20.6 kcal/mol). The relative stability of these product structures can again be explained by using

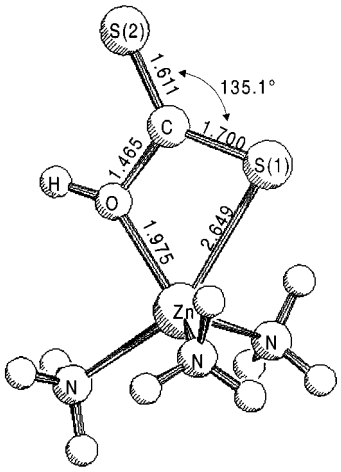


**Figure 3.** A minimum structure of the nucleophilic attack at the HF/3-21G* level of theory.

stereoelectronic effects. That **7** turns out to be the most stable species is the result of two oxygen lone pairs, which can engage in hyperconjugative interactions. In structure **6** a hydrogen is bound to the oxygen atom, which lowers the capability of the lone pair to interact with the antibonding orbitals of the C−S bond, leading to a less stable isomer. In structure **5** a hydrogen atom is bound to the oxygen too, and furthermore, the oxygen is in close contact with the zinc cation (2.864 Å, B3LYP). This leads to a strong interaction between the second lone pair of the oxygen atom and zinc, thus restraining the donating ability of the lone pair and resulting in an even less stable isomer. Due to the exhaustive investigations of the relevance of the Lindskog or Lipscomb mechanisms in most of the theoretical investigations given above,[25−32] we did not consider these reaction pathways but concentrated more on the stability of the resulting product structures. There is general agreement that neither mechanism does lead to a substantial energy barrier.

At the Hartree−Fock level using the small 3-21G* basis set all the above structures could be located. An additional minimum structure as depicted in Figure 3 was identified at this level of theory, coinciding with structural proposals in some works on carbonic anhydrase. This complex is very similar to structure **5**, but the zinc coordinates the OH group instead of the sulfur. However, this structure could not be reproduced using the more sophisticated 6-311+G* basis set. As an aside, we note that this result is not the consequence of using either polarization or diffuse basis functions, since already the parent 6-311G basis set gives this qualitative behavior.

In harmony with the results obtained for the conversion of $CO_2$,[32] the reaction path described above allows no formation of a hydration product structure with a zinc-bound protonated oxygen. However, as mentioned above, this conclusion is in sharp contrast to the hypothesis drawn in many previous works presented in the Introduction, where the coordination of zinc to the OH group was suggested.

The results of the 6-311+G* calculations are summarized in Table 2. As expected, the barriers decrease by switching from HF to B3LYP. This is due to the fact that the neglect of correlation energy in the HF model leads to larger errors for transition structures than for minimum structures. B3LYP, on the other hand, implicitly accounts for electron correlation and should therefore result in more reliable relative energies.

As a direct consequence of the large structural similarities between the geometries optimized at B3LYP/6-311+G* and HF/6-311+G*, the relative energies of B3LYP/6-311+G*

(59) Gonzales, C.; Schlegel, H. B.; *J. Chem. Phys.* **1989**, 90, 2154.
(60) Gonzales, C., Schlegel, H. B.; *J. Phys. Chem.* **1990**, 94, 5523.
(61) Fukui, K.; *Acc. Chem. Res.* **1981**, *14*, 363.
(62) Darensbourg, D. J.; Niezgoda, S. A.; Draper, J. D.; Reibenspies, J. H. *J. Am. Chem. Soc.* **1998**, *120*, 4690.

**Table 2.** Relative Energies for the Stationary Points of the Reaction of CA-Model Complexes with $CS_2$ as Depicted in Scheme 5[a]

| | **1 + 2** | **3** | **4** | **5** | **6** | **7** |
|---|---|---|---|---|---|---|
| | | | $[(NH_3)_3ZnOH]^+$ | | | |
| HF | 0.0 | −2.1 | 18.2 | −11.0 | −19.4 | −28.7 |
| B3LYP | 0.0 | −2.5 | 14.3 | −5.4 | −10.9 | −20.6 |
| B3LYP//HF | 0.0 | −2.1 | 14.5 | −4.3 | −9.5 | −19.8 |
| | | | $[(imidazole)_3ZnOH]^+$ | | | |
| HF | 0.0 | −5.8 | 15.4 | −15.4 | −17.8 | −31.1 |
| B3LYP//HF | 0.0 | −4.3 | 12.6 | −6.6 | −6.7 | −20.8 |

[a] All calculations employ the 6-311+G* basis set. Energies in kcal/mol, including ZPEs.

single-point calculations based upon HF/6-311+G*-optimized geometries are very similar to the results of direct B3LYP/6-311+G* optimizations. As documented in Table 2, the errors are between 0.2 and 1.4 kcal/mol. Hence, it seems that one can indeed use HF instead of B3LYP-optimized structures for obtaining reasonable B3LYP relative energies.

Furthermore, we have extensively tried to localize structures of an "inner sphere" reaction mechanism, starting with a bond formation between zinc and sulfur. However, no stable species indicating the existence of such a reaction path could be identified. All attempts to localize structures of this type at the HF or DFT level failed and lead to the formation of various encounter complexes of type **3** in Scheme 5 or resulted in the generation of structure **5**. The mechanism of the nucleophilic attack in the CA-catalytic reaction with $CO_2$ is thus retained for the case of $CS_2$, although the interaction between sulfur and zinc is strong.

**3.4. $CS_2$ Conversion through the Imidazole Complex.** The investigation of the larger imidazole complexes marked the limit of our computational capabilities. In particular, the geometry optimizations required a large number of iterations, and B3LYP optimizations became prohibitively expensive. However, as mentioned above, the B3LYP//HF single-point calculations acceptably agree with the B3LYP optimizations for the ammonia complexes. Hence, no B3LYP optimizations were carried out for the imidazole complexes. We rather based our study on B3LYP//HF single-point calculations on the HF-optimized structures, and relative energies given in the following refer to this level.

Selected structures optimized at HF/6-311+G* are displayed in Figure 4. Comparing the reactive imidazole complex **1** with its ammonia counterpart shows slightly shorter and stronger nitrogen metal bonds for the heterocyclic ligands (2.11 Å instead of 2.14 Å). This is due to the higher s character of its free electron pair. As a consequence, the zinc−oxygen bond is weakened, which increases the nucleophilicity of the oxygen. By this token the lower barrier of the nucleophilic attack (12.6 kcal/mol with respect to 14.5 kcal/mol at B3LYP//HF, see Table 2) can be explained. An encounter complex **3**, similar to the one displayed in Figure 2, was localized, stabilizing the reactants by 4.3 kcal/mol. The potential energy surface for the rotation of the $CS_2$ fragment around its $C_2$ axis is extremely flat. The activation energy amounts to only a few tenth of a kcal/mol.

Due to the prohibitively large computational costs, a minimum structure corresponding to the one displayed in Figure 3 for the ammonia model has not been sought extensively for the imidazole system. We assume that also in this case the nucleophilic attack results in the displacement of zinc-bound hydroxide by the sulfur atom S(1) (structure **5** in Scheme 5), combined with an energy gain of −6.6 kcal/mol. The Lindskog-like pathway leads next to the product structure **6**, which is stabilized by 6.7 kcal/mol with respect to the reactants, while the Lipscomb pathway yields also here a more stable product **7** with −20.8 kcal/mol.

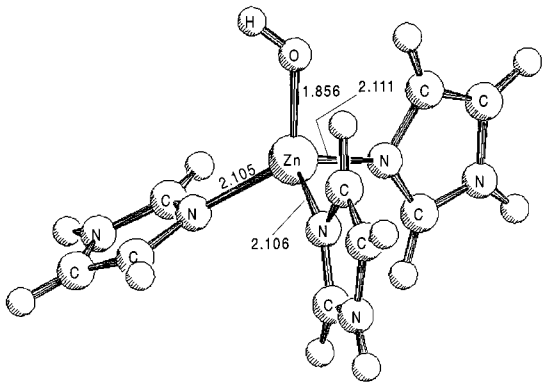


**1**

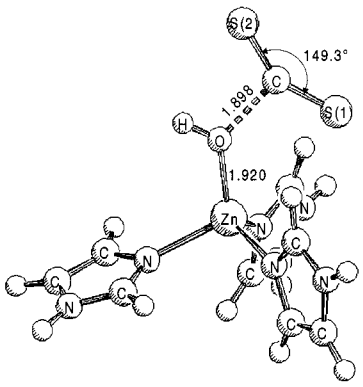


**4**

**Figure 4.** The imidazole reactant complex **4a** and the transition structure of the nucleophilic attack **4b** at the HF/6-311+G* level of theory.

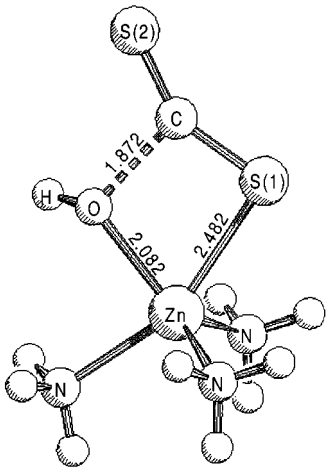


**Figure 5.** The inner sphere transition structure for the nucleophilic attack at the PM3-level.

**3.5. Further Notes and Comparison with $CO_2$ Conversion.** At first glance it would have seemed reasonable to postulate an "inner sphere" mechanism for the conversion of $CS_2$. In other words, the reaction would start by forming a bond between zinc and sulfur. The strong energetic interaction of $CS_2$ with zinc in the model calculations would support this hypothesis. Such structures could only be found using the semiempirical PM3 method; the transition structure for such a nucleophilic attack is displayed in Figure 5. However, the applicability of the PM3 method to zinc compounds is questionable, as pointed out by Bräuer et al.[63]

**Table 3.** Comparison of the Reaction of the Two CA-Model Complexes with $CS_2$ and $CO_2$ at the B3LYP/6-311+G*//HF/6-311+G* Level of Theory[a]

| | $[(NH_3)_3ZnOH]^+$ | | $[(imidazole)_3ZnOH]^+$ | |
|---|---|---|---|---|
| | $CO_2$ | $CS_2$ | $CO_2$ | $CS_2$ |
| 1 + 2 | 0.0 | 0.0 | 0.0 | 0.0 |
| 3 | −5.0 | −2.1 | −3.0 | −4.3 |
| 4 | 4.3 | 14.5 | 6.2 | 12.6 |
| 5 | −1.6 | −4.3 | −2.3 | −6.6 |
| 6 | −8.2 | −9.5 | −8.5 | −6.7 |
| 7 | −8.2 | −19.8 | −8.5 | −20.8 |

[a] Energies in kcal/mol, including ZPEs. Values for the $CO_2$ hydration are from Bräuer and Anders.[32]

Surprisingly, the mechanism of the conversion is identical for the reaction of $CO_2$ and $CS_2$ with CA-model complexes. For a comparison we summarized the results for both substrates in Table 3. As mentioned before, the decreased electrophilicity of $CS_2$ results in a higher activation energy for the nucleophilic attack. The differences amount to 10.2 kcal/mol for the $[(NH_3)_3ZnOH]^+$ model system and 6.4 kcal/mol for the imidazole complex (B3LYP/6-311+G*//HF/6-311+G*). Using either model complex a highly stabilized product **7** could be located, but in comparison to the $CO_2$ conversion the exothermicity of the reaction is increased by about 12 kcal/mol.

As Anders and co-workers reported,[32] solvent effects stabilize the reactants more than the products leading to an reversible reaction profile for the case of the CA-reaction with $CO_2$. We do not expect a very significant deviation of the solvation pattern for the reaction with $CS_2$. Our calculations therefore suggest the loss of reversibility of the reaction for this substrate. Nevertheless, an interesting field of stoichiometric reactions is conceivable for this type of reaction.

The most stable accessible products of this potential energy surface are complexes $[L_3ZnSH]^+$ with $L = NH_3$ or imidazole and COS molecules.[36] However, this is not the result of a desired reaction path. The investigation of the mechanism for their creation is not the goal of the present study, but it is conceivable that it contains a proton transfer and hence can be inhibited by the use of $[L_3ZnOR]^+$ complexes with $R \neq H$.

## 4. Summary

Quantum chemical calculations have been employed for the investigation of the reaction of CA-model complexes with $CS_2$. The model complexes $[(NH_3)_3ZnOH]^+$ and $[(imidazole)_3ZnOH]^+$ were used to compare the behavior of this new substrate to the conventional carbonic anhydrase reaction.

The uncatalyzed reaction with the hydroxide ion proceeds without an activation barrier in the gas phase. It is more exothermic due to the higher polarizability of sulfur, which allows for a better distribution of the charge in the molecule as compared to $CO_2$. The reaction of $CS_2$ with water shows the same features as in the $CO_2$ case. However, two opposing electronic effects that almost cancel each other are the reason for this behavior.

The catalyzed reaction is characterized by a higher activation barrier and an increased exothermicity. Thus, the reversibility of the reaction is lost due to strong zinc−sulfur interactions in the product structures. Three different product structures with experimental relevance could be localized. Despite the strong interaction of sulfur with zinc, we could find no evidence for an "inner sphere" reaction mechanism with precoordination of the substrate by a zinc−sulfur interaction.

**Acknowledgment.** Financial support by theDeutsche Forschungsgemeinschaft (Sonderforschungsbereich 436, University of Jena, Germany), the Fonds der Chemischen Industrie, and the Thüringer Ministerium für Wissenschaft, Forschung und Kultur (Erfurt, Germany) is gratefully acknowledged. In addition, we thank the Konrad-Zuse-Zentrum für Informationtechnik (Berlin) and the Hewlett-Packard Co. for providing us with CPU time. The authors thank Ulf Mazurek for technical support.

IC001149E

(63) Bräuer, M.; Kunert, M.; Dinjus, E.; Klussmann, M.; Döring, M.; Anders, E. *J. Mol. Struct. (THEOCHEM)* **2000**, *505*, 289.